

# Multi-stage LLC resonant converters designed for wide output voltage ranges

Chi-Wa, Tsang, University of Lincoln, UK, [ctsang@lincoln.ac.uk](mailto:ctsang@lincoln.ac.uk)  
C. Bingham, University of Lincoln, UK, [cbingham@lincoln.ac.uk](mailto:cbingham@lincoln.ac.uk)  
M.P. Foster, University of Sheffield, UK, [m.p.foster@sheffield.ac.uk](mailto:m.p.foster@sheffield.ac.uk)  
D.A. Stone, University of Sheffield, UK, [d.a.stone@sheffield.ac.uk](mailto:d.a.stone@sheffield.ac.uk)  
J. Leach, Castlet Ltd, [john.leach@castletltd.com](mailto:john.leach@castletltd.com)

## Abstract

The paper describes a novel multi-stage LLC resonant converter topology for facilitating wide output voltage ranges. This is achieved by combining the gain range of a capacitor-diode clamped LLC resonant converter with that of a traditional LLC resonant converter. A prototype converter is designed and commissioned to illustrate the design procedure and demonstrate resulting operational characteristics. Experimental results are used to show operational characteristics of the proposed converter.

## 1. Introduction

A challenge for many application sectors is the availability of controllable power converters that facilitate the production of wide output voltage ranges—the increasing use of high-power LED-based systems obtained through the connection of multiple low-power LEDs (in series or parallel configurations), provide a candidate example [1]. This is particularly acute when the full benefits of maintaining high efficiency across the voltage range is required [2].

Resonant converters have become increasingly popular candidates due to their soft-switching characteristics that reduce switching losses [3] and, as a result, improve the overall converter efficiency. While series and parallel resonant converters support the soft-switching characteristics needed for high efficiency, multi-resonant converters [3] have more favorable operating characteristics (e.g. narrow operating frequency). The LLC resonant converter, in particular, utilizes the parasitic elements found in a transformer to allow high power densities to be achieved. Nevertheless, one of the main impediments to their widespread adoption is that at their nominal operating point (the independent load point) an excessive current can flow if the load is not controlled, potentially leading to damage of both the converter and the load. A capacitor-diode clamp configuration has been considered in [5] to change the resonant converter characteristics by switching the resonant tank components, thereby facilitating a reduced voltage, and hence current, when subject to overloading conditions. The main advantage of the method in [5] in comparison to methods reported in [6][7] is that the output voltage is reduced autonomously without the need of any controller action.

This paper utilizes the unique gain reduction characteristic of the capacitor-diode clamped LLC resonant converter to allow a controllable wide output-voltage range to be achieved. A second LLC resonant converter is then connected in series with the first stage to further shape the current to produce the constant current characteristic, required in LED applications for instance.

## 2. Multi-stage LLC resonant converter

The schematic of the proposed converter is shown in Fig. 1, consists of two resonant converters connected in series. While both stages are of a LLC resonant converter type, the first stage has an additional capacitor-diode clamp.

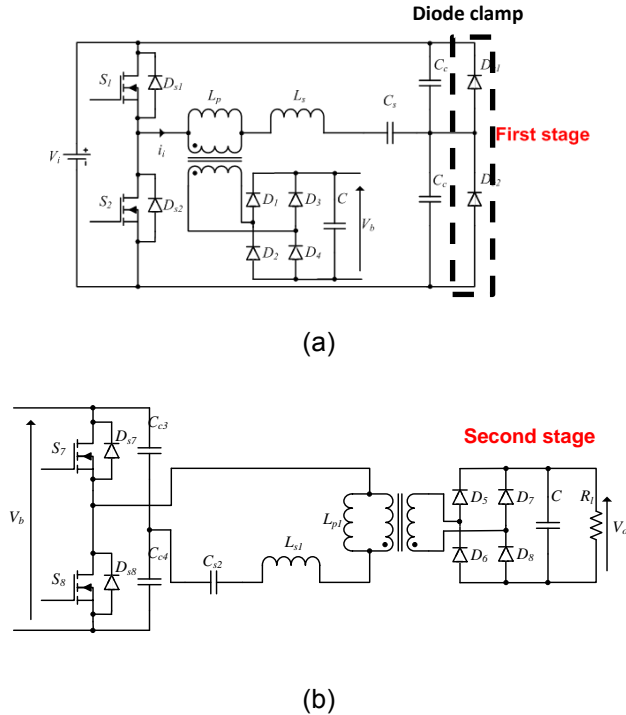


Fig. 1 Schematic diagram of the proposed converter. (a) First stage (b) Second stage

### 2.1. Converter's configuration

Three main functional parts are typically found in LLC resonant converters, viz. 1) a full- or half-bridge DC chopper which converts the DC input into a pulsed AC waveform, 2) a resonant tank which function is to block all but the fundamental component of the pulsed AC waveform to the output. The two inductors in the converter can be conveniently provided by the components of a transformer, which also provides galvanic isolation, and 3) a half- or full-bridge rectifier with a bulk capacitor which rectifies then smooths the waveform from the resonant tank to form a DC output.

A half-bridge DC chopper is chosen for the both converter stages in this instance, and is formed by MOSFET  $S_1$  and  $S_2$  for the first stage and by MOSFET  $S_7$  and  $S_8$  for the second stage. Resonant inductors,  $L_p$  and  $L_s$  of the first stage,  $L_{p1}$  and  $L_{s1}$  of the second stage, are the magnetizing and leakage inductances of the isolation transformers  $T_1$  and  $T_2$ , respectively.  $C_{c1}$ ,  $C_{c2}$ ,  $C_s$  and  $C_{c3}$ ,  $C_{c4}$ ,  $C_{s2}$  are the resonant capacitors of the first and second stage, respectively. The three resonant capacitors of each stage can be combined to form a single resonant capacitor using (1):

$$C_r = C_s + 2C_c \quad (1)$$

Diodes  $D_1$ ,  $D_2$ ,  $D_3$  and  $D_4$  form the full-bridge rectifier for the first stage. Similarly, diodes  $D_5$ ,  $D_6$ ,  $D_7$  and  $D_8$  form the full-bridge rectifier for the second stage. The internal body diodes  $D_{s1}$ ,  $D_{s2}$ ,  $D_{s7}$ ,  $D_{s8}$  are also shown in the figure, they are the critical components for zero voltage switching (ZVS) to take place.

Two additional diodes ( $D_{c1}$ ,  $D_{c2}$ ) across the resonant capacitors  $C_{c1}$ ,  $C_{c2}$  can be found in the first stage. These become active whenever the voltage across  $C_{c1}$ ,  $C_{c2}$  rises above the input

voltage or below zero volt, at which point the current is bypassed through the diodes, reducing the power transfer to the output, and hence reducing the effective gain without the need for any alteration in switching frequency.

### 3. Equivalent circuit model

With only the fundamental component of the input current passing through to the output, the equivalent circuit model of a non-capacitor-diode clamped (i.e. second stage) LLC resonant converter can be found using fundamental harmonic analysis (FHA) [3]. The magnitude of the input current ( $I_i$ ) and output voltage ( $V_o$ ) can be calculated using (2) and (3), respectively (n.b. ideal diodes are assumed and components parasitic resistances are neglected).

$$I_i = \frac{2V_i}{\pi Z_1} \quad (2)$$

$$V_o = \frac{\pi I_i (R_{eq} || sL_p)}{4n} \quad (3)$$

where  $Z_1 = R_{eq} || sL_p + sL_s + 1/sC_s + 1/2sC_c$ , is the input impedance of the resonant circuit and the load.  $s = j\omega_s$ , is the complex frequency and  $R_{eq} = 8n^2 R_l / \pi^2$  is the equivalent resistance presented by the rectifier, output filter and load reflected through the transformer;  $n$  is the transformer primary to secondary turns ratio.

With the capacitor  $C_c$  excited by a sinusoidal input current, its voltage at any given instant is found from (4). Substituting  $\omega_s t$  for  $\theta$  (where  $\omega_s = 2\pi f_s$  is the angular switching frequency), the capacitor voltage  $v_c$  at any  $\theta$  is then given by (5):

$$\begin{aligned} v_c(t) &= \frac{1}{2C_c} \int I_i \sin(\omega_s t) dt \\ &= -\frac{I_i}{2\omega_s C_c} \cos(\omega_s t) + V_n \end{aligned} \quad (4)$$

$$v_c(\theta) = -\frac{I_i}{2\omega_s C_c} \cos(\theta) + V_n \quad (5)$$

where  $V_n$  is the initial condition for a given conduction state starting at  $\theta = n$ .

Using (2) and (3), the output voltage for a given set of resonant tank components, load condition and operating frequency can be calculated. It is of benefit to be able to study the converter's voltage gain characteristics independently from the resonant tank component selection and input/output voltages. This can be achieved using the nominalized gain  $M_g$  which is obtained by substituting (2) into (3), and rearranging in terms of  $(2nV_o)/V_i$ , and then normalising against the three parameter: inductor ratio  $A = L_p/L_s$ , loaded quality factor  $Q = \sqrt{L_s/C_r}/R_{eq}$  and normalised switching frequency  $f_n = f_s/f_o$ . The result is given in (6):

$$M_g = \frac{2nV_o}{V_i} = \frac{A f_n^2}{A f_n^2 + f_n^2 - 1 + j(f_n^3 Q A - f_n Q A)} \quad (6)$$

Characteristics of the capacitor-diode clamped LLC resonant converter can also be found using FHA after the equivalent impedance of the clamped resonant capacitor is obtained. This involves the following three step procedure:

**Step 1:** obtain the piecewise equation describing the capacitor voltage under clamping conditions, shown in Fig. 2. The four equations covering each period are given in (7):

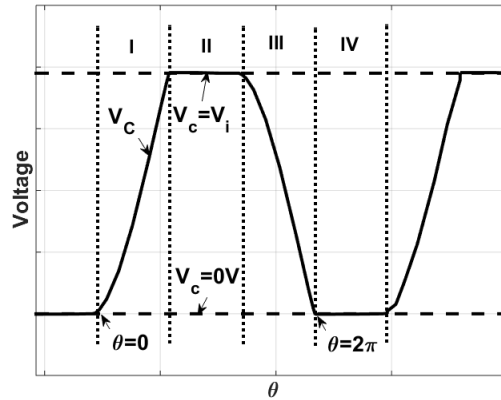


Fig. 2 Resonant capacitor voltage waveform under diode clamp conditions.

$$v_c(\theta) = \begin{cases} \frac{I_i}{2\omega_s C_c} (1 - \cos(\theta)) & 0 < \theta \leq \delta \\ V_i & \delta < \theta \leq \pi \\ V_i - \frac{I_i}{2\omega_s C_c} (1 + \cos(\theta)) & \pi < \theta \leq \pi + \delta \\ 0 & \pi + \delta < \theta \leq 2\pi \end{cases} \quad (7)$$

The diode-clamp non-conduction angle,  $\delta$ , is found by substituting  $v_c(\delta) = V_i$  into (7) and rearranging in term of  $\delta$ :

$$\delta = \cos^{-1} \left( 1 - \frac{2\omega_s C_c V_i}{I_i} \right) \quad (8)$$

**Step 2:** obtain the fundamental component of  $V_c$  using Fourier series, as in (9):

$$f(t) = a_0 + \sum_{n=1}^{\infty} (a_n \cos(n\omega_s t) + b_n \sin(n\omega_s t)) \quad (9)$$

$$a_0 = \frac{1}{2\pi} \int_{-T/2}^{T/2} f(t) dt$$

$$a_n = \frac{1}{\pi} \int_{-T/2}^{T/2} f(t) \cos(n\omega_s t) dt$$

$$b_n = \frac{1}{\pi} \int_{-T/2}^{T/2} f(t) \sin(n\omega_s t) dt$$

By substituting (5) into (7) the fundamental component of  $v_c$  is given by:

$$v_c(\theta) = \left[ \frac{2}{\pi} V_i \cos(\delta) + \frac{I_i}{2\pi\omega_s C_c} (1 + \cos(\delta) (\cos(\delta) - 2)) \right] \sin(\theta) \\ + \left[ -\frac{2}{\pi} V_i \sin(\delta) - \frac{I_i}{2\pi\omega_s C_c} (\delta + \sin(\delta) (\cos(\delta) - 2)) \right] \cos(\theta) \quad (10)$$

**Step 3:** obtain the equivalent impedance of the diode-capacitor combination using the transform  $\cos(\theta) = j\sin(\theta)$  and then dividing by resonant current, as follows:

$$Z_C = \left[ \frac{2V_i}{\pi I_i} \cos(\delta) + \frac{1}{2\pi\omega_s C_c} (1 + \cos(\delta) (\cos(\delta) - 2)) \right] + j \left[ -\frac{2V_i}{\pi I_i} \sin(\delta) - \frac{1}{2\pi\omega_s C_c} (\delta + \sin(\delta) (\cos(\delta) - 2)) \right] \quad (11)$$

With the equivalent impedance  $Z_C$  of the clamped capacitor identified, where the effect of the diode-clamp is accommodated, the input impedance of the capacitor-diode clamped LLC resonant converter is given by  $Z_2 = R_{eq} || sL_p + sL_s + 1/sC_s + Z_C$ . The magnitude of the resonant tank current under clamping is again found by FHA (12). The output voltage can be found by substituting (12) into (3).

$$I_i = \frac{2V_i}{\pi Z_2} \quad (12)$$

$$M_{g(\text{clmp})} = \frac{V_o}{V_i} 2n = \frac{R_{eq} || sL_p}{R_{eq} || sL_p + sL_s + \frac{1}{sC_s} + Z_C} \quad (13)$$

Since (12) cannot be solved analytically since  $I_i$  is unknown, and  $\delta$  and  $Z_C$  depend on  $I_i$ , an iterative procedure is employed, as follows: Firstly, estimate the resonant tank current  $I_i$  using (1), assuming the diode-clamp is inactive. Using this estimated value, the non-conduction angle,  $\delta$ , and capacitor-diode clamp equivalent impedance,  $Z_C$ , are estimated using (8) and (11). Next, instead of using (1) during the next iteration, using (12) for  $I_i$ , then (8) and (11) for the  $\delta$  and  $Z_C$  until convergence ensues.

Similar to the second stage, for the purpose of studying the voltage gain characteristic, the first stage converter gain,  $M_{g(\text{clmp})}$ , is obtained through substituting (12) into (3) and rearrange in terms of  $(2nV_o)/V_i$  as in (6), after which substituting  $s = j\omega$ ,  $Z_C = R + jX$  (where  $R$  and  $X$  are the real and imaginary part of  $Z_C$  in (11) respectively), and introducing the  $j\omega C_r$  term into both the numerator and denominator as in (14):

$$M_{g(\text{clmp})} = \frac{j^2 \omega^2 L_p C_r}{j^2 \omega^2 L_p C_r + \frac{j^3 \omega^3 L_s L_p C_r}{R_{eq}} + j^2 \omega^2 L_s C_r + \frac{j \omega L_p C_r}{C_s R_{eq}} + \frac{C_r}{C_s} + \frac{j^2 \omega^2 R L_p C_r}{R_{eq}} + R j \omega C_r + \frac{j^3 \omega^2 C_r X L_p}{R_{eq}} + j^2 X \omega C_r} \quad (14)$$

The final step involves substituting the following normalising factors  $L_p = AL_s$ ,  $L_s C_r = 1/\omega_0^2$ ,  $L_s/R_{eq} = Q/\omega_0$ ,  $f_n = \omega/\omega_0$  and  $B = C_r/C_s$ , to obtain:

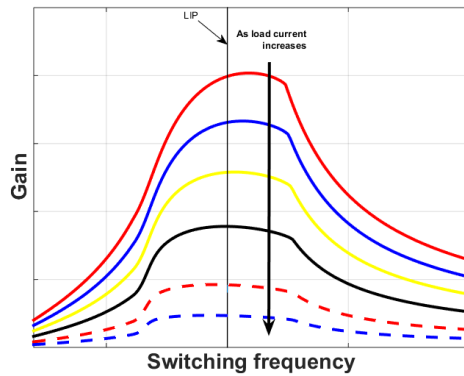
$$M_{g(\text{clmp})} = \frac{f_n^2 A}{f_n^2 A + f_n^2 - B + k_r + j(f_n^3 A Q - f_n A Q B + k_i)} \quad (15)$$

where  $k_r = \omega C_r (f_n A Q R + X)$  and  $k_i = \omega C_r (-R + f_n A Q X)$ , are terms accounting for the change in the effective impedance of the  $C_c$  caused by the diode-clamp when it is active, and it is assumed that the values for  $R$  and  $X$  have converged.

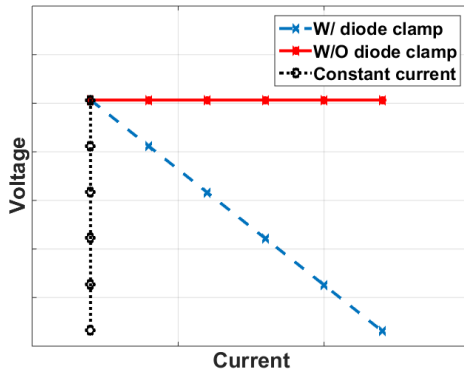
#### 4. Operation of the proposed converter

As part of the first stage (see Fig. 1 (a)), the capacitor-diode clamp limits the voltage across the resonant capacitor to reduce the overall voltage gain of the stage. Using (15), the gain of the clamped LLC resonant converter under different loading conditions at different operating frequencies can be found, as shown in the example Fig. 3 (a). Results show that as the current demand increases, the gain around the load independent point (LIP) reduces. The V-I characteristic at the operating point is given by the dashed-line in Fig. 3 (b).

The second stage (see Fig. 1 (b)) is included to shape the current of the first stage to that desired at the output. This stage is then operating at or above the resonant frequency (LIP) to achieve zero voltage switching (ZVS) and to reduce the required voltage gain range, since the gain reduces in a manner inversely proportional to the load—the desired constant current characteristic can therefore be obtained.



(a)



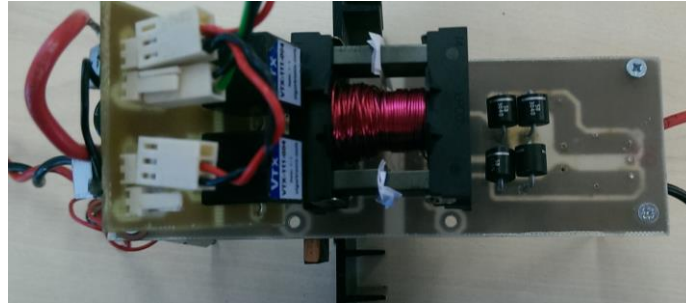
(b)

Fig. 3 Gain and V-I characteristics of the converter. (a) Gain characteristic of the first stage (b) V-I characteristic

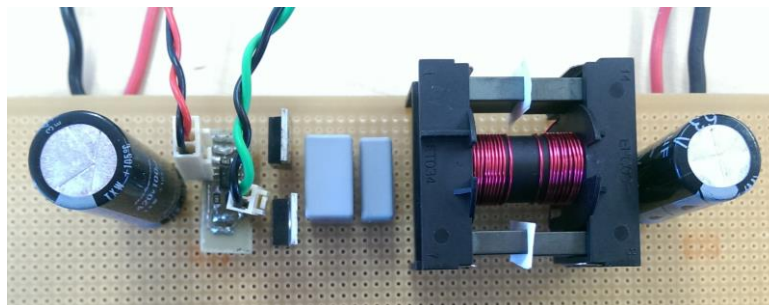
#### 5. Design example

A 20 W (12 V, 1.5 A) prototype is commissioned and built to demonstrate the operation of the proposed converter. Using (1), and with a chosen resonant frequency of 100 kHz and transformer turns ratio of 3:1, the resulting resonant tank components for the first stage are:  $L_p = 197 \mu H$ ,  $L_s = 39 \mu H$ ,  $C_{r1} = 32.5 nF$ . The second stage is also operating at the same switching frequency and its tank components are, by design,  $L_{p1} = 36 \mu H$ ,  $L_{s1} = 7 \mu H$ ,  $C_{r2} = 179 nF$ . The commissioned first and second stages of the converter are shown in Fig. 4 (a) and (b) respectively. Experimental measurements from the proposed converter are

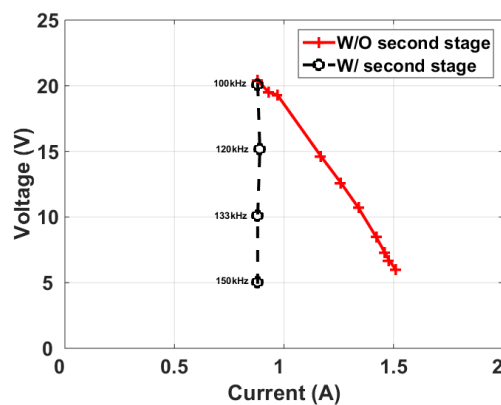
shown in Fig. 4 (c). The solid and dashed lines are the V-I characteristics of the first stage, and both stages, respectively; cf. Fig. 3 (b). The results show that the desired constant current characteristic can indeed be obtained by changing the switching frequency, hence the gain of the second stage. This makes it suitable for use in LEDs where the output current drawn is constant irrespectively of their different impedance.



(a)



(b)



(c)

Fig. 4 The V-I characteristics of the proposed converter. (a) first stage (b) second stage (c) P-I curve

## 6. Conclusion

This paper proposes connecting two LLC resonant converters in series to achieve a wide output voltage range. The first stage utilizes the unique characteristics of a diode-clamp to reduce the voltage gain found in a traditional LLC resonant converter, and hence the overload current. The second stage further shapes the current to obtain the desired constant current characteristic during normal operation. A design example is given and prototype built to show the feasibility of the proposed multi-stage converter, the results show that a constant current characteristic can be obtained, allowing the same current to be drawn by LEDs with different impedance.

## 7. Literature

- [1] Daek, J.-I., Kim, J.-K., Lee, J.-B., Youn, H.-S., Moon, G.-W., 'Integrated Asymmetrical Half-Bridge Zeta (AHBZ) Converter for DC/DC Stage of LED Driver with Wide Output Voltage Range and Low Output Current', IEEE Trans. Ind. Electron., 2015, 1 Vol. PP.
- [2] Musavi, F., Craciun, M., Gautam, D.S., Eberle, W., Dunford, W.G., 'An LLC Resonant DC-DC Converter for Wide Output Voltage Range Battery Charging Applications' IEEE Trans. Power Electronics., 2013, 5437-5445, Vol.28.
- [3] Steigerwald, R.L., 'A Comparison of Half-bridge Resonant Converter Topologies', IEEE Trans. Power Electron., 1988, pp. 174-182, Vol. 2.
- [4] Batarseh, I., 'Resonant converter topologies with three and four energy storage elements' IEEE Trans. Power Electron., 1994, pp. 66-73, Vol. 9.
- [5] Tsang, C.W., Foster, M.P., Stone, D.A., Gladwin, D.T., 'Analysis and Design of LLC Resonant Converters with Capacitor-Diode Clamp Current Limiting', IEEE Trans. Power Electronics., 2015, 1345-1355 Vol.30.
- [6] Gould, G.R. Bingham, C.M., Foster, M.P., Stone, D.A., 'CLL resonant converters with output short-circuit protection strategy', IEE Electric power applications, pp. 1296-1306, Vol, 152
- [7] Xie, X., Zhang, J., Zhao, C., Zhao, Z., Qian, Z., 'Analysis and optimization of LLC resonant converter with a novel over-current proection for LLC converter', IEEE Trans. Power Electronics., 2015, 435-443 Vol.30.